

## Conference Contribution

# LumiCal alignment system - Status report

Daniluk, W. (IFJPAN) *et al*

13 October 2014



The research leading to these results has received funding from the European Commission under the FP7 Research Infrastructures project AIDA, grant agreement no. 262025.

This work is part of AIDA Work Package 9: **Advanced infrastructures for detector R&D.**

The electronic version of this AIDA Publication is available via the AIDA web site  
<<http://cern.ch/aida>> or on the CERN Document Server at the following URL:  
<<http://cds.cern.ch/search?p=AIDA-CONF-2015-001>>

# LumiCal alignment system

## Status report

Witold Daniluk<sup>a</sup>, Beata Krupa<sup>a</sup>, Tadeusz Lesiak<sup>a</sup>, Arkadiusz Moszczyński<sup>a</sup>,  
Bogdan Pawlik<sup>a</sup>, Tomasz Wojtoń<sup>a</sup>, Leszek Zawiejski<sup>a,\*</sup>

<sup>a</sup>*Institute of Nuclear Physics PAN, Radzikowskiego 152, 31-342 Cracow, Poland*

---

### Abstract

The paper describes the status of the laser-based alignment-system for the luminosity detector, LumiCal, taking into considerations the conditions of the International Large Detector in the International Linear Collider project. The design of the system comprises two parts: the first one containing semi-transparent silicon sensors used to deliver simultaneous position measurements in the X,Y directions of the monitored object, and the second one in which the interferometric technique, i.e. the Frequency Scanning Interferometry (FSI), is proposed. Two laboratory prototypes for both components of the system were built and the preliminary measurements of the DUT displacements demonstrated their utility in the design of the final alignment system. The alignment of the LumiCal detector will allow us to monitor the detector displacements and possible deformations in its internal structure. Lack of information of the displacements will introduce a systematic effect which will have an impact on the accuracy of the final luminosity calculations. According to the requirements of the comprehensive research program prepared for the ILC, such a luminosity uncertainty should not be worse than  $10^{-3}$ .

*Keywords:* ILC, ILD , semi-transparent sensors, luminosity, laser, FSI technique

---

---

\* Corresponding author. Tel.: +48 12 662 8461; fax: +48 12 662 8012; e-mail: leszek.zawiejski@ifj.edu.pl.

## 1. Introduction

The discovery of the Higgs boson in the ATLAS [1] and CMS [2] experiments at the Large Hadron Collider (LHC) at CERN intensified the need to understand the whole complexity of its nature, together with its interactions and couplings to other particles. This need became a strong argument for the construction of the accelerator in which the colliding particles would be devoid of their internal structure to provide extremely precise measurements. Such a machine can help to understand deeper the Higgs boson, confirm possible further discoveries at the LHC and verify the theoretical models proposed to describe the phenomena beyond the Standard Model.

At present, there are three projects of the device in which  $e^+e^-$  collisions may take place: two for the linear collider: International Linear Collider (ILC) [3] and the Compact Linear Collider (CLIC) [4] and one for the circular collider, Future Circular Collider [5,6], with an option for  $e^+e^-$  collisions (FCCee). The most advanced in its development is ILC (both accelerator and detectors). The ILC research program requires that the luminosity measurement uncertainty should not be worse than  $10^{-3}$  ( $10^{-4}$  for Giga Z, a possible option of ILC operating in the energy range of the  $Z^0$  mass). This accuracy can be reached once the size of possible unwanted effects is known, which may worsen the accuracy of the luminosity calculations. For this reason these systematic effects should be monitored during the operation of the collider. One of such effects is related to possible displacements of the luminosity detector and a deformation of the internal detector structure. For ILC the integrated luminosity will be measured using a detector called LumiCal, which is one of the components of the main International Large Detector (ILD) [7], located at the very forward region, together with an other detector, BeamCal. In this report we describe the design of the proposed laser alignment system (LAS) for the LumiCal displacements as well as the first prototypes built for laboratory testing. The work on the LumiCal alignment is carried out within the framework of the FCAL international collaboration (Forward CALorimeters) [8,9]. The purpose of the FCAL collaboration is to develop the technology to build forward detectors for future experiments at ILC / CLIC.

## 2. LAS for LumiCal

The current design of the laser alignment system [9,10] proposed for the LumiCal detector contains two components:

- semi-transparent silicon sensors
- Frequency Scanning Interferometry (FSI)

Figure 1 shows the proposed design of the laser alignment system for the LumiCal detector.

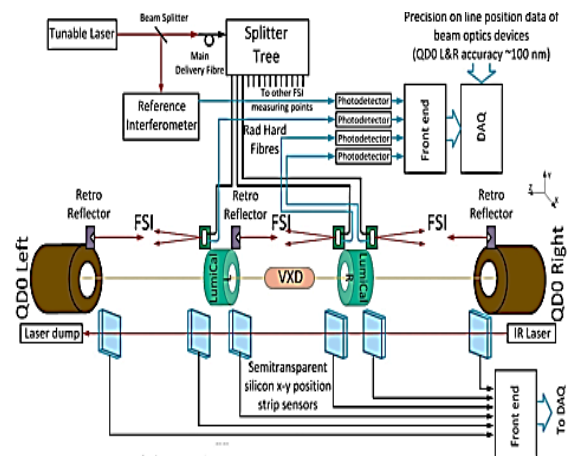


Figure 1. The design of the LAS for the LumiCal detector.

### 2.1. Position sensitive detector

To build a suitable prototype in the laboratory we have used several components that were previously employed in the ZEUS experiment [11-13]. The prototype contains semi-transparent sensors (STS) with readout cards and diode lasers supplied by the University of Oxford. The semi-transparent amorphous silicon sensors, DPSD-516, have light transmission above 85% for a laser beam with  $> 780$  nm within an active area of  $5 \times 5$  mm<sup>2</sup>, which allows several such sensors to be used in one laser beam. Each sensor contains 16 horizontal and 16 vertical strips (anode and cathode strips), whose signals (after pedestal subtraction) are used to determine the mean position of the sensor in the X and Y directions. Fig. 2 illustrates the schematic and actual shape of each individual sensor.

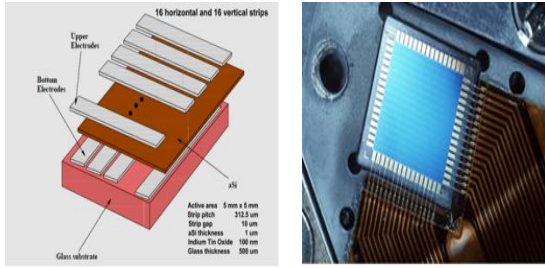


Figure 2. Left: The schematic diagram of the DSPD-516 sensor; Right: Real sensor linked with specially developed cables.

The details of the sensor structure and its properties can be found elsewhere [11,12]. All received DPSPD-516 sensors as well as their connecting cables were carefully tested under their correct electric properties and their response to laser beam light. The sensors that passed the selection were then used in the construction of one of the prototypes of the alignment system. The expected precision of position measurements performed using these sensors is about 10  $\mu\text{m}$ . The STS sensors system can be used to measure the LumiCal detector displacement over short distances, including the displacement of its internal sensor layers. It can also be used to determine the displacements of the LumiCal calorimeters related to the special reference frame, such as the QD0 focusing magnet, the last before the interaction point (IP). The semi-transparent sensors can be illuminated by lasers with power of about 5 mW. The special readout cables connect the sensors with the readout cards placed in the VME crate. The recovery of the VME system and re-installation of the LynxOS system allowed to incorporate a part of the old software used for collecting data from the strips.

## 2.2. Demonstration system and first data

Figure 3 shows a laboratory prototype of the system with six semi-transparent sensors attached to the optical table and readout system with the cards inside the VME crate.



Figure 3. Left: A demonstration prototype; Right: Cards of readout system inside the VME crate.

Figure 4 shows the beam profile signals (after subtraction of the pedestal value) from the X-strips of the subsequent sensors  $i$ . The mean positions,  $mX_i$ , were obtained from a Gaussian fit to the observed signals. Similar signals were visible for Y-strips.

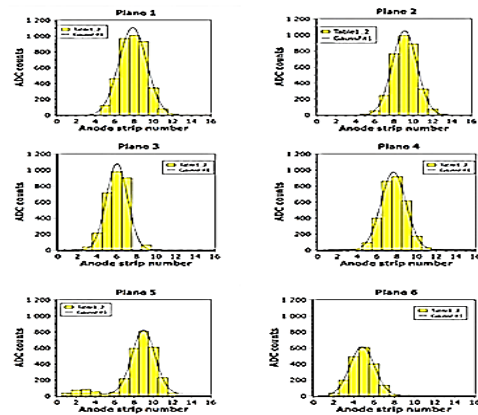


Figure 4. An example of beam profile signals from X-strips illuminated by the laser beam.

The coordinate system was oriented in such a way that the sensors 1 and 6 define the reference straight line (Fig. 5). Sensors 3 and 4 were mounted on the 2-D movable table.

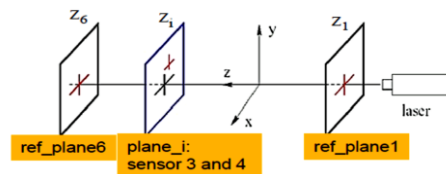


Figure 5. Geometry of the sensor system used to define the reference line and laser beam position calculation.

The calculation of the expected beam position at the sensor plane  $X_i$ ,  $Y_i$ , with the assumption that planes 1 and 6 are fixed, was done according to the formulae:

$$X_i = mX_1 (z_6 - z_i)/(z_6 - z_1) + mX_6(z_i - z_1)/(z_6 - z_1)$$

$$Y_i = mY_1 (z_6 - z_i)/(z_6 - z_1) + mY_6(z_i - z_1)/(z_6 - z_1),$$

where  $mX_i$  and  $mY_i$  represent the mean values of the beam position on the corresponding sensor plane. To reduce the fluctuation in the calculation of the beam position, the residual position of the beam line at each sensor was calculated as the distance from the expected position to the measured one (mean position):  $Rx_i = X_i - mx_i$  and  $Ry_i = Y_i - my_i$ .

As an example, Figure 6 shows the residuals of X-strips calculated from the preliminary set of data, related to the reference line defined by sensors 1 and 6. The second column illustrates the reduction of the fluctuations coming from the laser instability, when the laser worked continuously for a long period of time.

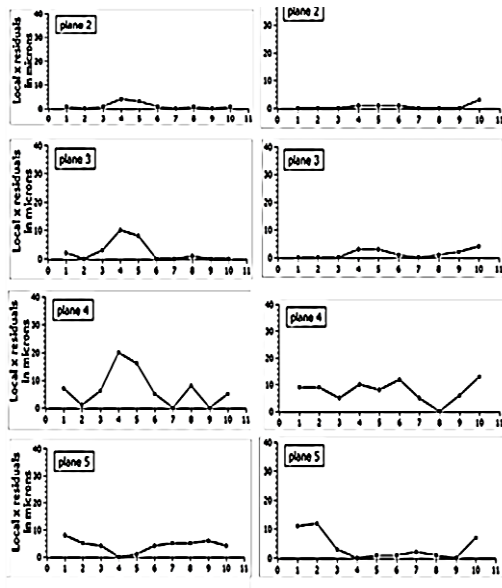


Figure 6.  $Rx_i$  residuals of the laser beam position for planes 2 – 5 as calculated in relation to reference straight line defined by 1 and 6 sensors. Left and right columns illustrate measurements for short and long time laser operation.

For a short-time measurement (when the laser was turned off after collecting a single set of data) the obtained accuracy of the laser beam mean position for the sensor did not exceed  $20 \mu\text{m}$ . The reduction to

smaller values of about  $10 \mu\text{m}$  was observed when the laser worked continuously for a long period of time.

### 2.3. Frequency Scanning Interferometry

Frequency Scanning Interferometry (FSI) technique was used as the second component of the LAS system for absolute distance measurement. FSI is based on a tunable laser and a frequency scan range  $\Delta\nu$ , using a Fabry-Perot (F-P) interferometer [14-20]. Two laser beams are split from one common beam (beam splitter) and directed towards the reference interferometer of known length and towards the interferometer whose length is to be measured. When the optical frequency of the laser is scanned continuously over the range of  $\Delta\nu$  for the interferometer with a fixed path, the phase  $\Delta\Phi$  as the difference of the phases of both beams (spatial parts of two electric fields) will change also continuously, resulting in the oscillations of the combined intensity of both beams with the number of  $\Delta N$  fringes given by:  $\Delta N = \Delta\Phi/(2\pi) = L \Delta\nu/c n$ , where  $c$  is speed of light,  $n$  is a refractive index of the propagation medium and the measured distance  $L$  is the optical path difference (OPD) between the reference and measured interferometers. Using a F-P with a free spectral range (FRS), the frequency scan range  $\Delta\nu$  can be defined as:  $\Delta\nu = r \text{ FRS}$ , with  $r$  as the number of FSR resonances detected during the  $\Delta\nu$  scan. Figure 7 shows the concept of a simple FSI setup with a single tunable laser and

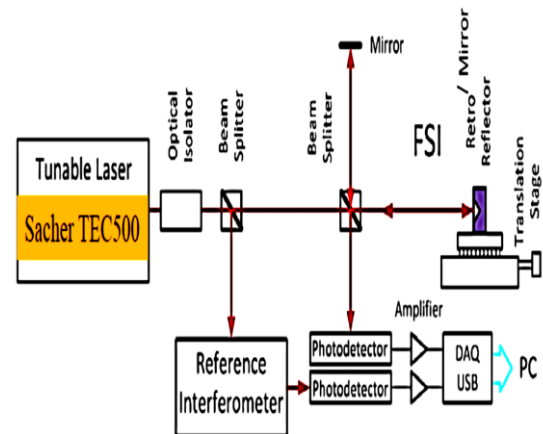


Figure 7. Schematic view of the FSI system with a single tunable laser.

Fig. 8 shows the implemented prototype. The setup is mounted on the SANDA optical table. The light source is a motorised Sacher Lion TEC500 tunable laser with



Figure 8. The experimental setup of a single laser FSI system.

a Littman/Metcalf system (output power up to 10 mW,  $659 \text{ nm} < \lambda < 672 \text{ nm}$ ). The F-P Thorlabs SA200 with a high-finesse ( $> 200$ ) is used to measure the frequency range scanned by the laser. The F-P has a free spectral range (FSR) of 1.5 GHz, leading to a spectrum of the signals with the distance between the two adjacent peaks equal to 0.002 nm (1.5 GHz). A Faraday Isolator (Thorlabs) was used to reject light reflected back into the laser cavity. After splitting by the beam splitters (BS), the laser beam was directed to the interferometers, the reference interferometer and the interferometer which was subject to measurement distance, and finally to the Thorlabs photodetector. The measured interferometer contains the retroreflector (or mirror) mounted on the translation stage. The output signals registered by the photodetector and F-P were analysed using an ADLINK DAQ-2010 card, capable of sampling simultaneously 4 channels at a rate of 2 MS/s/ch, working under the LabVIEW system. Figure 9 shows typical FSI (yellow) and F-P (blue) signals obtained with the prototype.

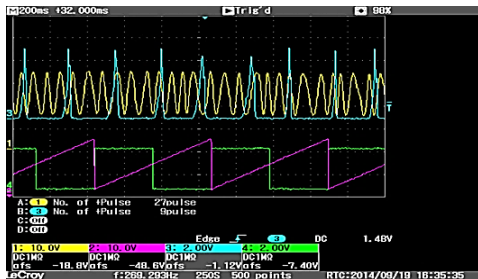


Figure 9. Typical signal view displayed by the oscilloscope.

## 2.4. First measurements

The experimental setup mounted on the optical table allows for measuring a distance within tens of centimeters. The maximal available  $\Delta\nu$  range during the frequency scan for the tunable laser is about 6 THz, which allows to measure the value  $\Delta N \sim 90000$  fringes for  $L = 50 \text{ cm}$ . Unfortunately, in practice this ideal situation was hard to take place. During tuning, the optical frequency laser showed discontinuities due to a “hop” between different single and multi-cavity modes. For this reason the scan of  $\Delta\nu$  had to include a number of shorter frequency scans (sub-scans). The number of fringes in these sub-scans was used further in the extrapolation procedure to get a dependence of  $\Phi$  vs.  $\nu$ . Another effect observed during the laser scan was connected with the motor head of the laser which created in the periodic way a strange structure in the signal amplitude of the registered fringes during the scan. This type of a defect requires an intervention of the manufacturer. The FSI and F-P signals visible on the display during the laser frequency scan often took a shape illustrated in Figs. 10 and 11. The mode-hop-free tuning range was often visible as an irregular structure in the F-P peaks. Figure 10 left shows the case of sub-scan which was used in the distance calculations and Figure 10 right illustrates the irregular structure of the F-P peaks. The amplitudes are indicated by dots for better identification.

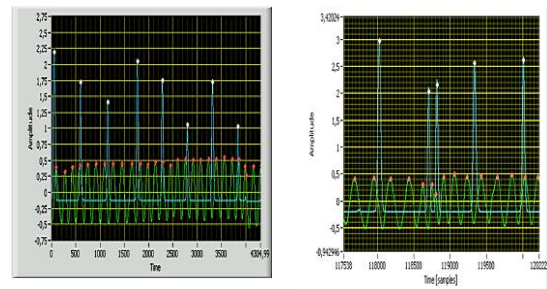


Figure 10. Left: An example of FSI and F-P signals from sub-scan with stable laser work; Right: Irregular structure of F-P peaks.

Figure 11 shows as an example the structure of amplitudes over the frequency scan  $\Delta\nu$  with segments of the stable laser work.

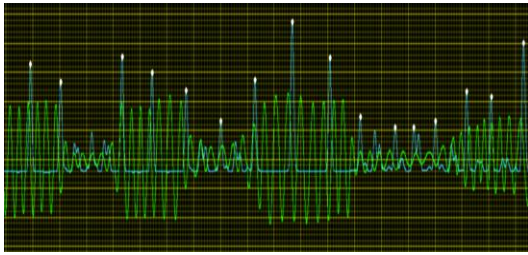


Figure 11. A structure of the amplitudes when optical frequency scan is made over  $\Delta\nu$ .

First measurements using the prototype have been performed in order to check the validity of the designed FSI system. In the case when an attempt was made to measure the distance in a continuous manner, over the whole range of  $\Delta\nu$ , large fluctuations of the final results with an uncertainty which reached even 1 mm were observed. For measurements performed in the narrow sub-scans the accuracy was much better; at distances of 30, 50 and 90 cm the measured uncertainties were 5, 6 and 15  $\mu\text{m}$ , respectively. Further advanced measurements and studies on the influence of the drift, vibration and temperature effects on the distance measurement accuracy will be possible after improving the quality work of the laser head motor.

### 3. Conclusions

The current design of the LumiCal laser alignment system is based on two techniques for measuring the relative and absolute distances. They use either infrared laser beam passing through the semi-transparent silicon sensors, giving the possibility of measuring simultaneously the positions in X, Y directions, or optical elements needed to build an interferometric system compatible with FSI principles. The basic element is a tunable laser. Besides the LumiCal displacement measurement, the system can be used to monitor the deformation of the detector's layers.

Two simple prototypes were built to test both. The preliminary measurements made with the help of both prototypes give hope to use these techniques in the future for the final alignment system.

Further advanced measurements with both components are necessary to design the details of the alignment system and to understand the impact of such effects as changes in temperature, vibration and drift on the accuracy of displacement measurements.

### Acknowledgments

This work is partly supported by: Commission under the FP7 Research Infrastructures project AIDA, grant agreement No.262025 and Polish Ministry of Science and Higher Education under agreement No. 2369/7.PR/2012/2.

### References

- [1] ATLAS Collaboration, G. Aad et al., Phys. Letters B 716 (2012) 1.
- [2] CMS Collaboration, S. Chatrchyan et al., Phys. Letters B 716 (2012) 30.
- [3] The International Linear Collider, Technical Design Report, ISBN 978-3-935702-78-2, ILC-Report-2013-040 (2013).
- [4] Compact Linear Collider, CLIC Conceptual Design Report: Volume 1,2, 3, CERN-2012-007, CERN-2012-003, CERN-2012-005.
- [5] The FCC-ee design study, <https://tlep.web.cern.ch>.
- [6] M. Bicer et al., JHEP01 (2014) 164.
- [7] The International Large Detector (ILD), <http://www.ilcild.org>.
- [8] FCAL Collaboration, H. Abramowicz et al., JINST 5 (2010) P12002.
- [9] FCAL Collaboration, H. Abramowicz et al., arXiv:1411.4924v2 [physics.ins-det], November 2014.
- [10] E. Banaś et al., Report No. 2071/PH, Institute of Nuclear Physics PAN, 2014, <http://www.ifj.edu.pl/pub1/reports/2014>.
- [11] T. Matsushita et al., Nucl. Instr. Meth. A 466 (2001) 383.
- [12] K. Korcsak-Gorzo et al., Nucl. Instr. Meth. A 580 (2007) 1227.
- [13] A. Polini et al., Nucl. Instr. Meth. A 581 (2007) 656.
- [14] A.F. Fox-Murphy et al., Nucl. Instr. Meth. A 383 (1996) 229.
- [15] S. M. Gibson et al., Optics and Lasers Engineering, 43 (2005) 815.
- [16] Hai-Jun Yang et al., Appl. Opt. 44 (2005) 3937.
- [17] Hai-Jun Yang et al., Nucl. Instr. Meth. A 575 (2007) 395.
- [18] A. Cabral et al., Proc. SPIE, Vol 7063, Interferometry XIV: Techniques and Analysis, 7063 (2008).
- [19] A. Cabral et al., Dimensional Metrology and

Frequency Sweeping Interferometry, Modern Metrology Concerns, ISBN: 978-953-51-0584-8, (2012), Chapter 3.

- [20] ATLAS Collaboration, G. Aad et al., JINST 9 (2014) P08009.